DALTON
FULL PAPER

Cation-directed syntheses of novel zeolite-like metalloaluminophosphates STA-6 and STA-7 in the presence of azamacrocycle templates

Paul A. Wright,*[a] Martin J. Maple,[a] Alexandra M. Z. Slawin,[a] Véronique Patinec,[a] R. Alan Aitken,[a] Simon Welsh[a] and Paul A. Cox[b]

[a] *School of Chemistry, University of St. Andrews, The Purdie Building, North Haugh, St. Andrews, Fife, UK KY16 9ST*
[b] *Centre for Molecular Design, University of Portsmouth, King Henry Building, King Henry I Street, Portsmouth, Hants, UK PO1 2DY*

Received 23rd November 1999, Accepted 13th March 2000
Published on the Web 30th March 2000

Hydrothermal syntheses of divalent metal cation-containing aluminophosphates, or MAPOs (M = Mg, Mn, Fe, Co or Zn), have been performed using the azamacrocycle 1,4,8,11-tetramethyl-1,4,8,11-tetraazacyclotetradecane as a structure directing agent. Whereas STA-6 (*St. A*ndrews-6), a small pore zeotype with a one-dimensional channel system, is prepared when magnesium, manganese or iron is included in the synthesis gel, a new solid, STA-7, is prepared in the presence of cobalt or zinc. The structure of STA-7 has been solved and found to possess a tetrahedrally connected framework with a fully three-dimensional interconnected small pore channel system. The organic template molecules included during synthesis can completely be removed without loss of framework integrity from the cobalt form. Syntheses using the hexaazamacrocycle 1,4,7,10,13,16-hexamethyl-1,4,7,10,13,16-hexaazacyclooctadecane have also been successful in preparing STA-7 in the presence of divalent metal cations. Both STA-6 and STA-7 structure types can be considered to be built up of cages and chemical analysis and computer simulation suggest strongly that the macrocycles act to template these cages.

Introduction

The synthesis of novel microporous framework solids, such as zeolites and aluminophosphates, continues to generate new possibilities in adsorption and catalysis. Most of the new structures[1] owe their origin to the inventive use of quaternary ammonium salts and amines as structure-directing agents, or templates. Tertiary amines are particularly effective templates for aluminophosphate molecular sieves. Recent work has broadened the range of such amines used in synthesis to include the oxaaza-cryptand 4,7,13,16,21,24-hexaoxa-1,10-diazabicyclo[8.8.8]hexacosane ('Kryptofix 222') and the azamacrocycle 1,4,8,11-tetramethyl-1,4,8,11-tetraazacyclotetradecane (tmtact), both of which contain tertiary nitrogens within a ring system. This has resulted in crystallisation of the tetrahedrally co-ordinated aluminophosphate $AlPO_4$-42[2] and the magnesioaluminophosphate STA-6,[3] respectively. These are both best described as cage structures where the macrocycles occupy the cages unbound. This is in direct contrast to the gallophosphate structure that is formed using 1,4,8,11-tetraazacyclotetradecane ('cyclam') as a template, in which the macrocycle is bound to the framework.[4] The well developed chemistry and wide variety of azamacrocycles suggests they may be used to template a range of possible structures, and in this report we describe the further use of 'tmtact' and 1,4,7,10,13,16-hexamethyl-1,4,7,10,13,16-hexaazacyclooctadecane (hmhaco) in the synthesis of metal-substituted aluminophosphates.

In particular, we have compared the products of hydrothermal syntheses performed in the presence of different cations that are able to substitute for aluminium in the tetrahedral framework of the aluminophosphates. Incorporation of divalent cations frequently results in the crystallisation of structure types different from those that result from purely aluminophosphate gel compositions (in the presence of the same organic template). For example, the DAF-1 structure type has only been prepared with the aluminium partially substituted by divalent cations such as magnesium and cobalt, the aluminophosphate analogue having yet to be prepared (the $AlPO_4$-5 structure crystallises instead).[5] Importantly, the incorporation during synthesis of divalent cations introduces potentially active sites for shape selective acid catalysis[5] and when transition metals such as manganese, iron and cobalt are incorporated the resultant solids show catalytic activity and shape selectivity for the partial oxidation of alkanes in the presence of air under relatively mild conditions.[6]

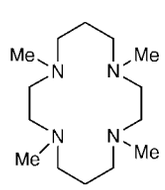

1

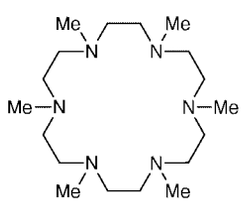

2

We show below that the use of azamacrocycles directs the synthesis of novel divalent metal-substituted framework structures STA-6 and STA-7. Furthermore, we have found that the type of divalent cation determines which of the two framework structures forms. To our knowledge, this is the first example of structure direction in such structures by the type of cation in the gel; typically a single structure type results from the incorporation of divalent cations into a framework type (this is the case, for example, for the Mg, Co, Mn and Zn forms of MAPO-36[7]). To investigate the role of azamacrocycles in these syntheses we have performed computer simulation of their inclusion within the pore systems of STA-6 and STA-7 and also investigated their thermal stability upon template removal.

Experimental

Homogeneous gels of composition x R:0.2 $M(OAc)_2$:0.8

DOI: 10.1039/a909249h

This journal is © The Royal Society of Chemistry 2000

Table 1 Details of syntheses using tmtact and hmhaco as templates. All preparations were heated at 190 °C for 48 hours, and gel concentrations are given in the text

Cation ratio in synthesis gel	Azamacrocycle	Product solid (by XRD)	Unit cell contents (from TGA, ICP-AES)	C:H:N	
				calculated	measured
1.0 Al:1.0 P	tmtact (R′)	$AlPO_4$-21			
0.2 Mg:0.8 Al:1.0 P	tmtact	Mg–STA-6	$(Mg_{0.2}Al_{0.8}PO_4)_{16}\cdot 1.5R'\cdot 2.5H_2O$[3]		
0.2 Mn:0.8 Al:1.0 P	tmtact	Mn–STA-6			
0.2 Fe:0.8 Al:1.0 P	tmtact	Fe–STA-6			
0.2 Co:0.8 Al:1.0 P	tmtact	Co–STA-7	$(Co_{0.2}Al_{0.8}PO_4)_{24}\cdot 2.3R'\cdot 9H_2O$	10.1:2.48:3.36	10.5:2.35:3.34
0.2 Zn:0.8 Al:1.0 P	tmtact	Zn–STA-7	$(Zn_{0.2}Al_{0.8}PO_4)_{24}\cdot 2.6R'\cdot 10H_2O$	10.9:2.71:3.66	10.7:2.48:3.24
1.0 Al:1.0 P	hmhaco (R″)	$AlPO_4$-21			
0.2 Mg:0.8 Al:1.0 P	hmhaco	MgAPO-36, Mg–STA-7			
0.2 Co:0.8 Al:1.0 P	hmhaco	Co–STA-7	$(Co_{0.2}Al_{0.8}PO_4)_{24}\cdot 2.0R''\cdot 7H_2O$	10.9:3.24:4.24	10.3:2.64:4.15

$Al(OH)_3$:1.0 H_3PO_4:4000 H_2O, where R is the template (for tmtact $x = 0.5$, for hmhaco $x = 0.3$) and M^{2+} the cation substituting for aluminium (M = Mg, Mn, Fe, Co or Zn), were prepared and heated at 190 °C for 40–48 hours in polytetrafluoroethylene (PTFE)-lined autoclaves. In a typical gel synthesis for Co–STA-7, 0.19 g of cobalt acetate tetrahydrate was dissolved in a solution of 0.39 g of phosphoric acid in 15 cm^3 of distilled water. A gel was prepared by addition of 0.29 g of hydrated aluminium hydroxide and to this 0.5 g of the tmtact template was added. Magnesium, manganese, iron, cobalt and zinc acetates, aluminium hydroxide and the amines were obtained from Aldrich and used as supplied. In each case the synthesis pH was 7. For comparison, syntheses without divalent cations and with M:P ratios of 0.15 and 0.25:1 were also performed under similar conditions. The resultant crystalline products of hydrothermal synthesis were filtered off, washed with distilled water and dried. Where there was a range of different particle sizes the coarser fraction, which often contained single crystals of dimensions suitable for single crystal diffraction, was physically separated from the rest of the sample.

X-Ray powder diffraction patterns of all products were collected on a Philips diffractometer using Cu-Kα radiation and operating in Bragg–Bentano geometry with a secondary monochromator. This enabled phase identification. For structural analysis of the Co– and Zn–STA-7 phases the samples were loaded into quartz glass capillaries and analysed on STOE diffractometers operating in Debye–Scherrer geometry with primary monochromation with Fe-$K_{\alpha 1}$ and Cu-$K_{\alpha 1}$ X-radiation, respectively. For cobalt-containing samples the use of Fe-$K_{\alpha 1}$ X-radiation is preferable to the more widely available Cu-$K_{\alpha 1}$ X-radiation because there is no simultaneous X-ray fluorescence. Selected crystals were examined by single crystal diffractometry.

CCDC reference number 186/1897.

See http://www.rsc.org/suppdata/dt/a9/a909249h/ for crystallographic files in .cif format.

The organic content of the solids was examined by a Carlo Erba CHN elemental analyser. To confirm the template was included intact, the inorganic framework was dissolved in 5 M HCl and the solution analysed by NMR. For magnesium and zinc containing solids a sample of the microporous solid (*ca*. 50 mg) was added to 5 M HCl (0.3 cm^3) and left for 12 h to allow complete dissolution. The resulting clear colourless solution was transferred to an NMR tube and a solution of sodium 3-trimethylsilylpropanesulfonate in D_2O (0.2 cm^3) added. For cobalt-containing samples a similar dissolution procedure resulted in a clear pink solution. This was made basic by addition of 2 M sodium hydroxide solution and then extracted with CH_2Cl_2 (3 × 2 cm^3). The solvent was evaporated and the colourless oily residue dissolved in 5 M hydrochloric acid (0.3 cm^3) which was transferred to an NMR tube and examined in the same way as the other samples. ^{13}C NMR spectra were recorded at 75 MHz using a Bruker AM300 instrument on solutions in 5 M hydrochloric acid/D_2O using sodium 3-trimethylsilylpropanesulfonate as reference; chemical shifts are reported in ppm to high frequency of the reference. (The shifts described here are therefore correctly referenced to an internal standard, and these values should be taken in place of those recorded in the absence of an internal standard and reported in reference 3.) The inorganic content of pure phases was determined by inductively coupled plasma atomic emission spectroscopy (ICP-AES). The materials were dissolved in concentrated nitric acid prior to analysis.

Thermogravimetric analysis was performed by heating finely ground samples in an oxygen flow at 5 °C min^{-1} to 620 °C and holding this temperature for one hour. Carefully to remove all the template and measure the pore volumes the samples were calcined in flowing dry oxygen at 560 °C and then cooled under dry flowing nitrogen. Freshly calcined samples were stabilised against exposure to atmospheric moisture by cooling to room temperature under n-hexane vapour. Pore volumes were measured volumetrically using dinitrogen at 77 K. Before measurement of the pore volume of the calcined and stabilised sample the n-hexane was removed by heating to 400 °C under a vacuum of 10^{-3} Torr.

To model the likely position of the tmtact molecule within the STA-6 and STA-7 solids prepared using this azamacrocycle as a template a computational approach combining Monte Carlo docking and subsequent Simulated Annealing was adopted. The pH of synthesis favours the dicationic form of the template, and literature suggests the most stable form would be that with the two protons on alternating nitrogens in the ring system,[8] so this dication was used in the modelling. In order to ensure charge neutrality in the calculation, an additional charge of −2 was distributed evenly across the anionic component of the framework. The cations were assigned half their formal charge. Periodic boundary conditions were applied and the framework atoms held fixed at their experimental positions. The energy and conformation of the template within the pore structure was determined using a Simulated Annealing method in which the template was heated for 1000 time steps of 1×10^{-15} s at 750, 600, 450, 300 and finally 200 K prior to energy minimisation. Calculations were performed using the CVFF Constant Valence Force Field within the program Discover.[9] We have assumed that short-range interactions between the framework and the template will be dominated by the larger oxygen ions and have omitted short range terms between the cations and the template. The possible location of the hmhaco template in the STA-6 and STA-7 topologies was examined in a similar way. For this template a tricationic form was used, with positive charges on alternate nitrogens.

Results

Synthesis

The results of the syntheses are given in Table 1. Notably the synthesis of the STA-6 and STA-7 phases only occurs in the presence of divalent cations. For the aluminophosphate gel

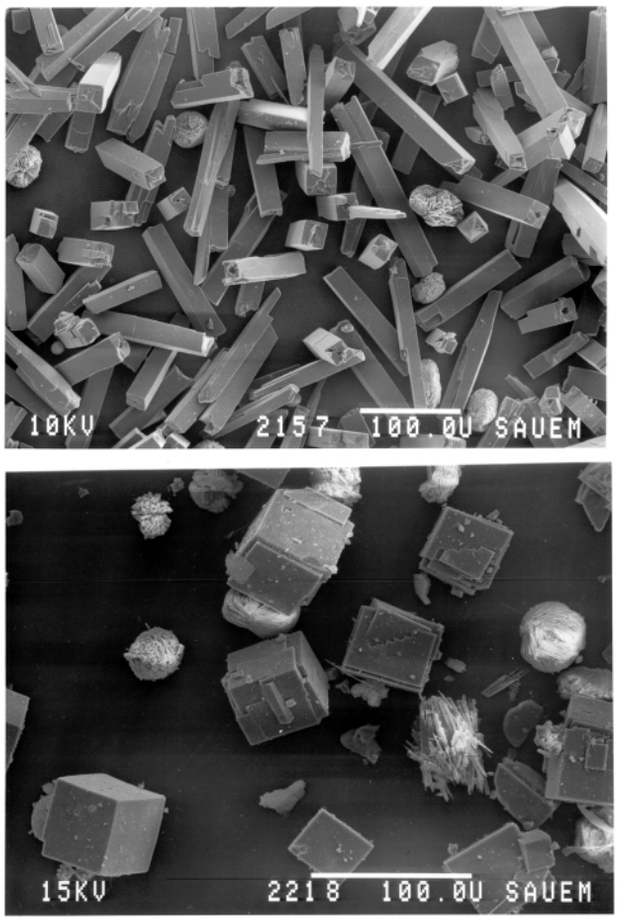

Fig. 1 Scanning electron micrographs of the magnesioaluminophosphates Mg–STA-6 prepared with tmtact (above) and Mg–STA-7 prepared with hmhaco (below).

composition in the presence of tmtact or hmhaco $AlPO_4$-21 is formed. For those syntheses using tmtact in the presence of divalent cations the crystallisation of the STA-7 phase results from the presence of cobalt or zinc in the synthesis gel, whereas the presence of magnesium, manganese or iron results in the formation of STA-6. Using hmhaco, magnesium results in the crystallisation of a mixture of fine needles of MgAPO-36 and some larger crystals of Mg–STA-7, whereas cobalt results in the crystallisation of Co–STA-7. The purest samples of Co–STA-7 and Zn–STA-7 are prepared for both templates from gels with M^{2+}:P ratios of 0.20:1. Higher or lower contents of divalent cations result in crystalline impurities. In typical preparations using tmtact and hmhaco, yields of 50–60% on phosphorus were obtained for STA-7 prepared in the presence of cobalt and zinc. Much lower yields (a few percent) were obtained using magnesium as the divalent cation.

Whereas Mg–STA-6 is formed in the presence of tmtact as needle-like tetragonal prisms (Fig. 1, top), Mg–STA-7 (prepared in the presence of hmhaco) crystallises with pseudo-cubic morphology, and dimensions close to 100 μm (Fig. 1, bottom), in low yield, in a mixture dominated by crystals of MgAPO-36. In the presence of both tmtact and hmhaco, Co–STA-7 crystallises as elongated tetragonal prisms up to 200 × 100 × 100 μm in dimensions, with the 'cobalt blue' coloration typical of cobalt aluminophosphates with cobalt(II) in tetrahedral coordination. Zn–STA-7 (prepared with tmtact) also crystallises as slightly elongated tetragonal prisms with dimensions 50 × 25 × 25 μm. Whereas Co– and Zn–STA-7 can be prepared pure, and can therefore be characterised fully, Mg–STA-7 is prepared as a minor fraction and can only be characterised by single crystal crystallography.

Table 2 Crystallographic details for as-prepared samples of STA-7 containing different metal cations in the framework. For unit cell compositions see Table 1

	Mg–STA-7	Co–STA-7	Zn–STA-7
Azamacrocycle, R	hmhaco	tmtact	tmtact
Crystal system	Tetragonal	Tetragonal	Tetragonal
Space group	*P*4/*n*	*P*4/*n*	*P*4/*n*
μ/mm^{-1}	0.573	11.75	1.394
a/Å	18.7732(8)	18.740(5)	18.691(2)
c/Å	9.4537(5)	9.439(7)	9.423(1)
V/Å^3	3331.8(3)	3314.9(25)	3292.0(6)
T/K	293	293	150
Z	8	8	8
R(int)	0.0712	0.079	0.0635
Unique reflections	2403	2472	4743
Observed (>2σ(*F*))	1629	1311	3851
R_1	0.0539	0.1169	0.0912
$wR_2(F^2)$	0.1422	0.3134	0.2203
Average (Al,M)–O/Å	1.769	1.718	1.767
E.s.d. of (Al,M)–O bond lengths	0.017	0.020	0.020
Average P–O/Å	1.515	1.562	1.514
E.s.d. of P–O bond lengths	0.007	0.014	0.007

Crystallography

Single crystals of Mg–STA-7 (hmhaco), Co–STA-7 (tmtact) and Zn–STA-7 (tmtact) from the preparations described above were shown to possess the same framework topology by single crystal X-ray diffraction experiments at St. Andrews and at station 9.8 at the Daresbury laboratory, as detailed in Table 2. The basic framework structure was solved for each material using the SHELXS package and refined fully anisotropically in *P*4/*n* using SHELXL.[10] It was not possible to identify template molecules unambiguously from the difference Fourier syntheses, because they will necessarily be disordered, as the symmetry of the template is lower than that of the framework. For the hmhaco templated Mg–STA-7, electron density peaks in the large cages were attributed to disordered carbons and nitrogens of the template and those in the smaller cages to water molecules, consistent with analytical and modelling data. For tmtact templates, where modelling using the diprotonated cations had been carried out, modelled positions for the carbons and nitrogens of the template were used to account for extra-framework scattering. In the space group *P*4/*n* the aluminium sites (which contain aluminium plus the divalent metal) and the P sites are able to achieve full ordering. The difference in bond lengths between the two kinds of sites is clear for all structures. For the Mg– and Zn–STA-7 samples the 'Al' sites have an average Al–O bond length of 1.77(2) Å and the phosphorus sites have a mean bond length of 1.515(7) Å. For the Co–STA-7 there appears to be slightly less ordering (bond lengths of 1.72(2) Å for 'Al'–O and 1.56(1) Å for P–O) which may indicate that there are domains within the crystal with ordering arrangements of opposite phase.

To confirm that the single crystals of Co– and Zn–STA-7 were representative of the as-prepared bulk samples, powder diffraction profiles collected in capillary mode using the STOE diffractometers were matched using the Rietveld refinement method within the GSAS suite of programs.[11] The profiles of the Zn– and Co–STA-7 samples prepared with tmtact were fitted satisfactorily using the single crystal framework structure of STA-7 at 293 K with a disordered template in the modelled position as a starting point, and allowing the framework atom positions to vary within tight constraints. A reasonable final fit (R_{wp} = 16.3%, R_p = 12.2%) indicated that no diffraction peaks extra to those from the STA-7 were present, and confirmed the bulk samples are phase pure. Unit cell parameters of a = 18.732(2) and c = 9.417(1) Å were obtained

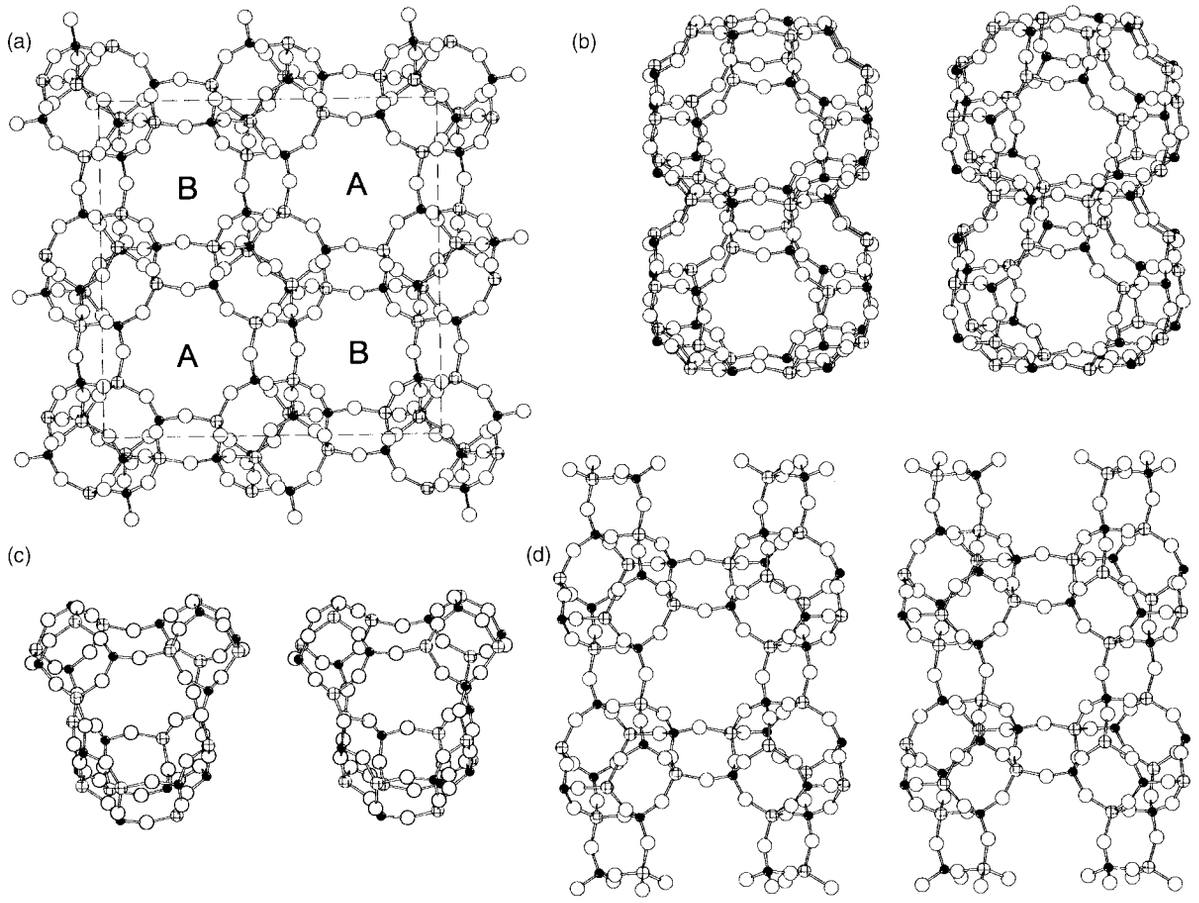

Fig. 2 Illustrative diagrams of the STA-7 structure, with Al as hatched spheres, P as black spheres and O as white spheres. Projection down the *c* axis reveals the presence of two distinct pore systems, A and B. The A system is made up of cages linked along *c* through 8MRs (b), whereas the B system is made up of smaller interconnecting spaces, (c). The framework can be considered as sheets made up of double 6MRs linked parallel to *c* by 4MRs (d).

for the Co–STA-7 and $a = 18.709(2)$ and $c = 9.428(1)$ Å for the Zn–STA-7.

The structure is fully tetrahedrally co-ordinated and, like STA-6 and $AlPO_4$-42, the other zeotypes templated by azamacrocycles, can best be considered as having a pore structure made up of cages. The *c*-axis projection (Fig. 2a) shows the arrangement of two distinct channel systems (denoted A and B), each constrained by rings containing eight tetrahedral cations and eight oxygens, so-called eight-membered rings (8MRs). The A channels are composed of cages, linked *via* planar 8MRs (3.9 Å in free diameter), stacked along *c* as shown in Fig. 2(b). The cages also possess four elliptical 8MR openings to the B channel system, each opening having dimensions of 4.3 × 3.7 Å. The B channels (Fig. 2c) are connected along *c via* 8MR windows 3.5 Å in free diameter and to the A channel system *via* the elliptical 8MRs. The framework itself may be considered as being made up of chains of double 6MRs (hexagonal prisms) linked along *c* by single 4MRs and linked to each other by Al–O–P bonds (Fig. 2d).

Chemical analysis

NMR analysis of organic compounds liberated from the aluminophosphate-based samples by dissolution in acid and comparison with NMR of the azamacrocycles as obtained from Aldrich reveals that the macrocycles are included intact in STA-6[3] and STA-7, but are not fully intact in the Mg–STA-7/MgAPO-36 product of experiments with hmhaco. (For tmtact in acid δ_C 52.0, 47.1, 45.4, 19.6; for hmhaco at pH 1 δ_C 53.2, 44.8; for extract from Co–STA-7 with tmtact δ_C 52.0, 47.3, 45.4, 20.2; for extract from Co–STA-7 with hmhaco δ_C 53.7, 45.3; for extract from Mg–STA-7/MgAPO-36 mixture prepared with hmhaco δ_C 53.9, 53.1, 49.8, 45.9, 45.4, indicating template decomposition has occurred.)

It is possible to arrive at a unit cell composition of the as-prepared Co– and Zn–STA-7 samples prepared by combining the results of TGA, carbon, hydrogen and nitrogen (CHN) analysis, inorganic ICP-AES analysis and crystallography. TGA in oxygen shows endothermic weight loss below 175 °C, which can be attributed to desorption of water, and exothermic weight loss between 200 and 620 °C, resulting from template removal (Table 1). Combining these data for the Co–STA-7 sample prepared with tmtact (R′), for example, indicates a unit cell composition $(Co_{0.2}Al_{0.8}PO_4)_{24}\cdot 2.3R'\cdot 9H_2O$. For the sample of Co–STA-7 prepared with hmhaco (R″), the unit cell composition is $(Co_{0.2}Al_{0.8}PO_4)_{24}\cdot 1.96R''\cdot 7H_2O$. Elemental CHN analysis is reasonably consistent with compositions arrived at in this way.

Molecular modelling

The numerical results of computations to determine the non-bonding energies of the azamacrocycles within the pores of STA-6 and STA-7 frameworks are given in Table 3.

For tmtact in STA-7 the energies show that the molecule very significantly favours the larger A cage in STA-7 over the inter-cage regions. The computer modelled location of the tmtact template in STA-7 is illustrated in Fig. 3. The template molecule is very strained in the smaller cage and the high energy suggests that it is too big to be accommodated at this location. There are two of the larger cages per unit cell and therefore we would predict that there can be two templates per unit cell in these sites. The slightly higher calculated CHN contents may indicate that small fragments are trapped within the B pore system. The

Table 3 Minimised non-bonded energies for the tmtact and hmhaco templates in different sites within the pores of STA-6 and STA-7 (calculated by Monte Carlo docking and Simulated Annealing procedures, see text for details)

Template	Structure	Site	Non-bonding energy/kJ mol^{-1}
tmtact	STA-6	Cage	−50.1
hmhaco	STA-6	Cage	742.2
tmtact	STA-7	A cage	−31.2
tmtact	STA-7	B cage	485.5
hmhaco	STA-7	A cage	−9.7
hmhaco	STA-7	B cage	2002.9

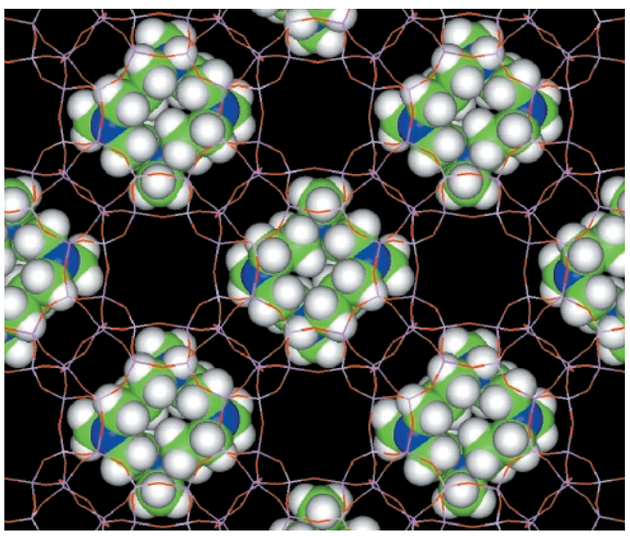

Fig. 3 The modelled position of the lowest energy location of the tmtact molecular cation within the A type cages of STA-7, viewed down *c* (determined by Monte Carlo docking followed by Simulated Annealing).

results for the energies of hmhaco in STA-7 show a similar pattern. The larger template has a less favourable non-bonded energy in the A cages of STA-7 than the tmtact template, indicating that the molecule is a slightly poorer 'fit' to the cavity than the tmtact molecule. In the smaller cage the non-bonded energy for this larger molecule is much more unfavourable than for tmtact.

The tmtact and hmhaco molecules within the cages of STA-6 show very large differences in their non-bonded energies. Whereas the tmtact molecule fits well into the STA-6 cage (as indicated by the ready formation of STA-6 in the presence of Mg, Mn and Fe), the hmhaco molecule is very strained in the STA-6 cage, as reflected by the very high non-bonding energy.

Thermal stability and porosity of STA-7

Calcination of the STA-7 materials in oxygen results in complete removal of the template. Whereas magnesium- and zinc-containing solids become white after calcination in oxygen, Co–STA-7 turns green, indicating at least part of the cobalt(II) is converted into cobalt(III). Adsorption of n-hexane results in the solid becoming blue again, indicating the cobalt is reduced to cobalt(II).[12] To confirm that the calcined sample of Co–STA-7 retained the framework structure, the X-ray profile was examined by Rietveld refinement. Using the as-prepared framework as a starting model, and refining with framework bond lengths and angles constrained to chemically reasonable values, gave an excellent fit to the data ($a = 18.5738(12)$, $c = 9.3634(7)$ Å, $R_{wp} = 9.1\%$, $R_p = 6.8\%$) and confirmed that the framework is retained intact (Fig. 4). Removal of the template results in a decrease of cell volume from 3304.6(8) Å^3 (measured from powder data) to 3230.2(4) Å^3. Nitrogen adsorption measurements on the calcined Co–STA-7 reveal a pore volume of 0.25 cm^3 g^{-1}, considerably higher than that measured for calcined Mg–STA-6 (0.13 cm^3 g^{-1}) and much closer to the values measured for other microporous solids containing three-dimensionally connected pores. Calcination of Zn–STA-7 results in transformation of part of the solid to a dense phase *via* an amorphous phase while some of the STA-7 framework remains intact.

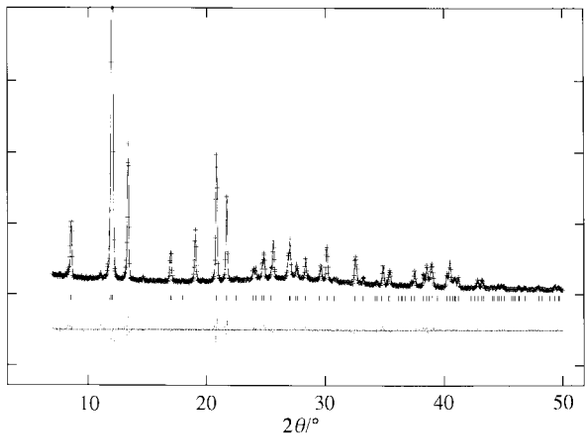

Fig. 4 Rietveld profile fit and difference plot of Co–STA-7, calcined at 560 °C in flowing oxygen to remove the template. The pattern is plotted with the ordinate scale up to 50% of the maximum intensity of the major peak. The close agreement of experimental profile (crosses) and simulated pattern (solid line) ($R_{wp} = 9.1\%$, $R_p = 6.8\%$) indicates the tetrahedrally connected framework is retained intact, with space group *P*4/*n* and $a = 18.5738(12)$, $c = 9.3634(7)$ Å.

Discussion

STA-7, which is prepared in the presence of cobalt or zinc using tmtact and in the presence of cobalt or magnesium using hmhaco, is a very interesting addition to the aluminophosphate family of structures, being the first zeotype containing two distinct and fully interconnected small pore channel systems.

Although it is not possible from diffraction experiments to locate unambiguously the template molecules (which exhibit disorder and statistical occupancy), the chemical composition suggests that there are probably 2 molecules per unit cell for STA-7 prepared in the presence of both tmtact and hmhaco, plus some additional organic amine fragments and water. Molecular modelling indicates that the sites in the cages in the A channel system are energetically highly favoured over sites in the B channel system for both types of azamacrocycle used to direct the synthesis, suggesting that the macrocycles template the formation of these cages. The A cages of STA-7 are compared with those of STA-6 (also templated by tmtact) and with those of the aluminophosphate $AlPO_4$-42 that has the LTA (zeolite A) framework topology, templated by the 'Kryptofix 222' cryptand (Fig. 5). The cages in STA-7 are 9.4 Å high with a free diameter of *ca*. 10.0 Å in the *ab* plane, compared to corresponding values of 10.4 Å high and 9.0 Å in free diameter for STA-6. The modelling results indicate that whereas the hmhaco can be located within the STA-7 structure, its larger size results in it being unable to be located within the slightly smaller cages of STA-6.

The structure-directing effect of the divalent metal cation on the product of syntheses using tmtact (magnesium, manganese or iron giving STA-6; cobalt or zinc, STA-7) is, to our knowledge, unique, and we are currently investigating the underlying mechanism. Also, it is notable that whereas both azamacrocycles template STA-7 in the presence of cobalt, gels containing magnesium give STA-6 in the presence of tmtact and MgAPO-36 (and some STA-7) in the presence of hmhaco. Computer simulation suggests that the reason that STA-6 is not produced

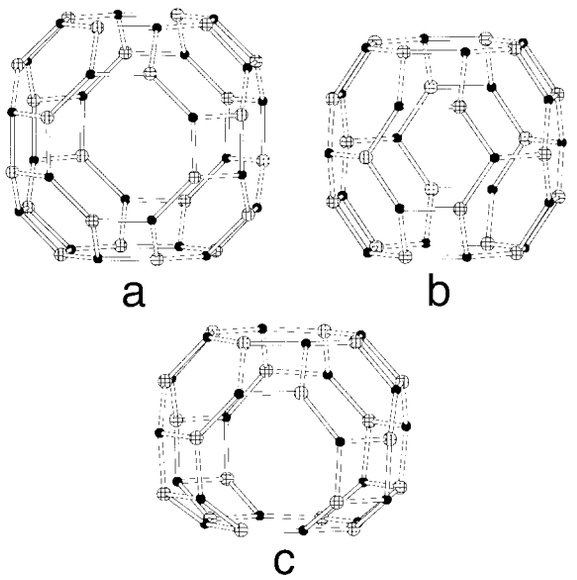

Fig. 5 Comparison of cages templated by azamacrocycles in the aluminophosphates (a) $AlPO_4$-42, (b) STA-6 and (c) STA-7. For clarity, only the tetrahedral cations are represented in the diagram, and oxygens are omitted.

with the larger azamacrocycle is simply because the template cannot be accommodated within the STA-6 cage. Competitive crystallisation of the MgAPO-36 solid, which takes up fragments of amines resulting from thermal breakdown of the azamacrocycles, then gives the mixture of products that is observed.

Removal of the template from STA-7 results in a 2.3% decrease in unit cell size. The colour changes upon calcination of Co–STA-7 and adsorption of n-hexane upon cooling are consistent with the cobalt being at least partially oxidised to cobalt(III), and remaining in the framework, followed by subsequent reduction back to cobalt(II). The pore volume of the calcined material (0.25 $cm^3\ g^{-1}$) is comparable with that of other zeolites and aluminophosphates with three-dimensional pore systems.

The future use of azamacrocycles as templates is likely to produce a range of novel aluminophosphate structures. On the basis of the experimental results to date, azamacrocycles with tertiary nitrogens are expected to produce tetrahedrally connected frameworks with structures based on cages. Removal of the templates produces solids with high porosity that are of interest as adsorbents and catalysts. In addition, the inclusion of 'functional' molecules *unbound*, and therefore with the potential ability to co-ordinate cations, may give solids with interesting redox and cation exchange properties.

Acknowledgements

Drs Simon Teat and Philip Lightfoot and Mr David Wragg are thanked for help in collecting data on station 9.8 at Daresbury and Dr Alistair Robertson and Professor Peter Bruce for help with the laboratory X-ray diffractometry. Dr Irvine Davidson is thanked for providing the SEM micrographs. We very gratefully acknowledge the support of EPSRC (V. P., P. A. W.) and BP Amoco (CASE award for M. J. M).

References

1 W. M. Meier, D. H. Olson and Ch. Baerlocher, *Atlas of Zeolite Structure Types*, Elsevier, London, 4th edn., 1996.
2 L. Schreyek, F. D'Agosto, J. Stumbe, P. Caullet and J. C. Mougenel, *Chem. Commun.*, 1997, 1241.
3 V. Patinec, P. A. Wright, P. Lightfoot, R. A. Aitken and P. A. Cox, *J. Chem. Soc.*, *Dalton Trans.*, 1999, 3909.
4 T. Wessels, L. B. McCusker, Ch. Baerlocher, P. Reinert and J. Patarin, *Microporous Mesoporous Mater.*, 1998, **23**, 67; D. S. Wragg, G. B. Hix and R. E. Morris, *J. Am. Chem. Soc.*, 1998, **120**, 6822.
5 P. A. Wright, C. Sayag, F. Rey, D. W. Lewis, J. D. Gale, S. Natarajan and J. M. Thomas, *J. Chem. Soc.*, *Faraday Trans.*, 1995, 3527.
6 J. M. Thomas, R. Raja, G. Sankar and R. G. Bell, *Nature* (*London*), 1999, **398**, 227.
7 P. A. Wright, S. Natarajan, J. M. Thomas, R. G. Bell, P. L. Gai-Boyes, R. H. Jones and J. Chen, *Angew. Chem.*, *Int. Ed. Engl.*, 1992, **31**, 1472.
8 M. Micheloni, A. Sabatini and P. Paoletti, *J. Chem. Soc.*, *Perkin Trans. 2*, 1978, 828; M. Micheloni, P. Paoletti and A. Vacca, *J. Chem. Soc.*, *Perkin Trans. 2*, 1978, 945.
9 Discover 3.1 program, MSI, San Diego, CA, 1993.
10 G. M. Sheldrick, SHELXS, University of Göttingen, 1986; SHELXTL, version 5.3, Program for the solution of crystal structures, University of Göttingen, 1993.
11 A. C. Larson and R. B. von Dreele, Generalized Crystal Structure Analysis System, Los Alamos National Laboratory, USA, 1988.
12 J. M. Thomas, G. N. Greaves, G. Sankar, P. A. Wright, J. Chen, A. J. Dent and L. Marchese, *Angew. Chem.*, *Int. Ed. Engl.*, 1994, **33**, 1871.